# Supporting Information

## Kuroda et al. 10.1073/pnas.1002178107

### SI Methods

**Monoclonal Antibodies Against Nox4.** Generation of the anti-Nox4 mouse monoclonal antibody (3D2), which detects Nox4 and does not cross-react with Nox2, has been described (1).

**Immunoblot Analyses.** Homogenates of heart, kidneys, liver, and aorta were prepared in RIPA lysis buffer containing 50 mmol/L Tris (pH 7.5), 150 mmol/L NaCl, 1% IGEPAL CA-630, 0.1% SDS, 0.5% deoxycholic acid, 10 mmol/L $Na_4P_2O_7$, 5 mmol/L EDTA, 0.1 mmol/L $Na_3VO_4$, 1 mmol/L NaF, 0.5 mmol/L 4-(2-aminoethyl) benzenesulfonyl fluoride hydrochloride (AEBSF), 0.5 μg/mL aprotinin, and 0.5 μg/mL leupeptin. Samples were subjected to SDS/PAGE. Proteins were transferred onto polyvinylidene fluoride microporous membranes (BioRad) and probed with primary antibodies. These include monoclonal antibodies raised against Nox4 and polyclonal antibodies raised against Nox1 (Santa Cruz), Nox2 (Abcam), Nox3 (Santa Cruz), and $p22^{phox}$ (Santa Cruz).

**RT-PCR.** Expression of $p22^{phox}$ mRNA was evaluated by RT-PCR with specific primers as follows: ATGGGGCAGATCGAGTGGGC (forward primer) and TCACACGACCTCATCTGTCA (reverse primer).

**DHE Staining.** After harvest, heart tissues were immediately embedded in optimum cutting temperature (OCT) compound in ethanol–dry ice and stored at −80 °C. Unfixed frozen samples were cut into 5-μm thick sections and placed on glass slides. DHE (10 μmol/L) was applied to each tissue section, and then the sections were coverslipped. The slides were incubated in a light-protected humidified chamber at 37 °C for 30 min. Ethidium fluorescence (excitation at 490 nm, emission at 610 nm) was examined by fluorescent microscopy (2).

**TAC.** TAC was performed according to the method published previously (3).

**Echocardiography.** Mice were anesthetized with 12 μL/g of body weight of 2.5% avertin (Sigma), and echocardiography was performed with ultrasonography (Acuson Sequoia C256; Siemens Medical Solutions USA Inc.). A 13-MHz linear ultrasound transducer was used. The 2D guided M-mode measurements of the LV internal diameter were taken from three or more beats and averaged. LV end diastolic dimension was measured at the time of the apparent maximal LV diastolic dimension, and LV end systolic dimension was measured at the time of the most anterior systolic excursion of the posterior wall.

**Histological Analyses.** The LV accompanied by the septum was cut into base, midportion, and apex, fixed with 10% formalin, embedded in paraffin, and sectioned at 6-μm thickness.

For Nox4 expression, the sections were stained using the anti-Nox4 antibody (clone 3D2). For 8-OHdG staining, the sections were incubated in 3% $H_2O_2$ in PBS to prevent endogenous peroxidation and blocked with 5% BSA in PBS. Anti–8-hydroxy-2′-deoxyguanosine (anti–8-OHdG) antibody (Oxis International Inc.) was diluted to 7.5 μg/mL in PBS and applied to the sections for 1 h at 37 °C. After washing, biotinylated secondary antibody (anti-mouse IgG; BD Pharmingen) was applied for 1 h, followed by streptavidin-HRP (BD Pharmingen) for 30 min at room temperature. The myocyte cross-sectional area was measured from images captured from the sections stained using WGA. The outlines of 100–200 myocytes were traced in each section. Interstitial fibrosis was evaluated by Masson trichrome staining (4). Apoptosis was evaluated as DNA fragmentation detected in situ using TUNEL staining.

**$H_2O_2$ Measurement.** $H_2O_2$ production was measured with an Amplex Red $H_2O_2$ assay kit (Molecular Probes; Invitrogen) according to the manufacturer's instructions. In brief, left ventricular blocks (30–50 mg) were incubated with Amplex Red (100 μmol/L) and horseradish peroxidase (1 U/mL) for 30 min at 37 °C in Krebs–Hepes buffer protected from light. The supernatant was then transferred to a 96-well plate, and absorbance was measured (560 nm). Background fluorescence, determined in a control reaction without sample, was subtracted from each value. $H_2O_2$ release was calculated using $H_2O_2$ standards and expressed as micromoles per milligram of dry tissue.

**Measurement of Mitochondrial Superoxide Derived from Succinate.** Mitochondrial fractions were suspended in 200 μL assay buffer. After preincubation with 5 μmol/L lucigenin, succinate was added to a final concentration of 10 mmol/L. The chemiluminescence was continuously monitored using a luminometer and antimycin A was added to a final concentration of 100 μmol/L.

**Assays for Measurement of Oxidative Stress.** Mitochondrial fractions containing equal amounts of proteins (25 μg) were assessed for aconitase activity (Aconitase-340; Oxis International Inc.) and MDA or MDA+4-HAE content (LPO-586; Oxis International Inc.) according to the manufacturer's instructions.

**Mitochondrial Swelling Assay.** Fifty micrograms of isolated mouse heart mitochondria from c-$Nox4^{-/-}$ and WT mice subjected to either TAC or sham operation were suspended in swelling buffer (250 mmol/L sucrose, 10 mmol/L Mops, 5 μmol/L EGTA, 2 mmol/L $MgCl_2$, 5 mmol/L $KH_2PO_4$, 5 mmol/L pyruvate, and 5 mmol/L malate) and incubated with 150 μmol/L calcium chloride ($CaCl_2$) in a final volume of 200 μL in a 96-well plate for 20 min. Absorbance was read at 520 nm.

**Quantitative Real-Time PCR for Mitochondrial DNA.** The mtDNA content was quantified by real-time PCR of cardiac DNA as described (5). Primer sequences for *cytochrome b* and β-*actin* are as follows: CCACTTCATCTTACCATTTATTATCGC (forward primer) and TTTTATCTGCATCTGAGTTTAA (reverse primer) for *cytochrome b*; CTGCCTGACGGCCAGG (forward primer) and CTATGGCCTCAGGAGTTTTGTC (reverse primer) for genomic β-*actin*.

**ATP Production Assay.** The mitochondrial fraction of mouse hearts was prepared as described above. ATP production was measured with an ATP Bioluminescent Assay kit (Sigma).


1. Ago T, et al. (2009) Upregulation of Nox4 by hypertrophic stimuli promotes apoptosis and mitochondrial dysfunction in cardiac myocytes. *submitted*.
2. Ago T, et al. (2004) Nox4 as the major catalytic component of an endothelial NAD(P)H oxidase. *Circulation* 109:227–233.
3. Zhai P, et al. (2006) An angiotensin II type 1 receptor mutant lacking epidermal growth factor receptor transactivation does not induce angiotensin II-mediated cardiac hypertrophy. *Circ Res* 99:528–536.
4. Matsuda T, et al. (2008) Phosphorylation of GSK-3α is essential for myocyte proliferation in the heart under pressure overload. *Proc Natl Acad Sci USA* 105:20900–20905.
5. Duncan JG, Fong JL, Medeiros DM, Finck BN, Kelly DP (2007) Insulin-resistant heart exhibits a mitochondrial biogenic response driven by the peroxisome proliferator-activated receptor-alpha/PGC-1alpha gene regulatory pathway. *Circulation* 115:909–917.

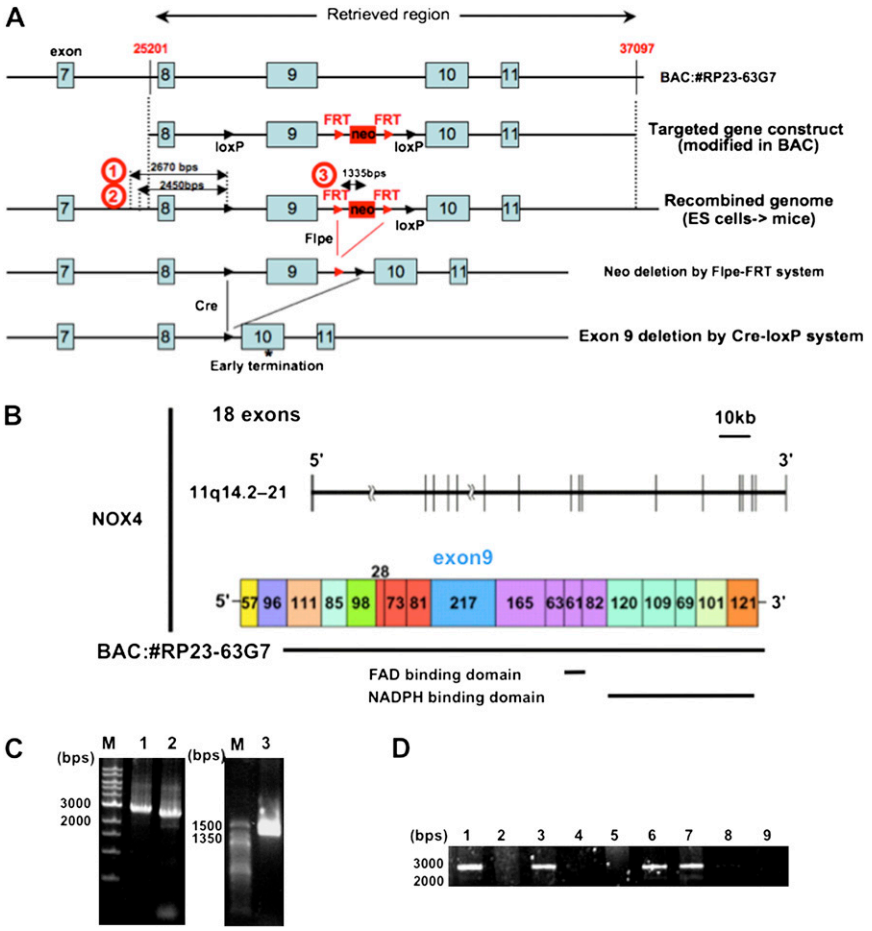


**Fig. S1.** Generation of c-*Nox4*$^{-/-}$ mice. (*A* and *B*) Design of the *Nox4* targeting construct and the genomic structure of the Nox4 gene. We inserted loxP sites to delete the entire exon 9, which allows early termination in exon 10, resulting in truncation of the region including the FAD- and NADPH-binding domains. Note that this means complete destruction of Nox4 function and is equivalent to complete deletion of Nox4 protein. (*C*) PCR of the genomic DNA in ES cells confirming recombination. Bands 1–3 correspond to DNA fragments indicated in *A*. (*D*) Germ-line transmission of the recombinant allele was confirmed (lanes 1, 3, 6, and 7 are flox/+).

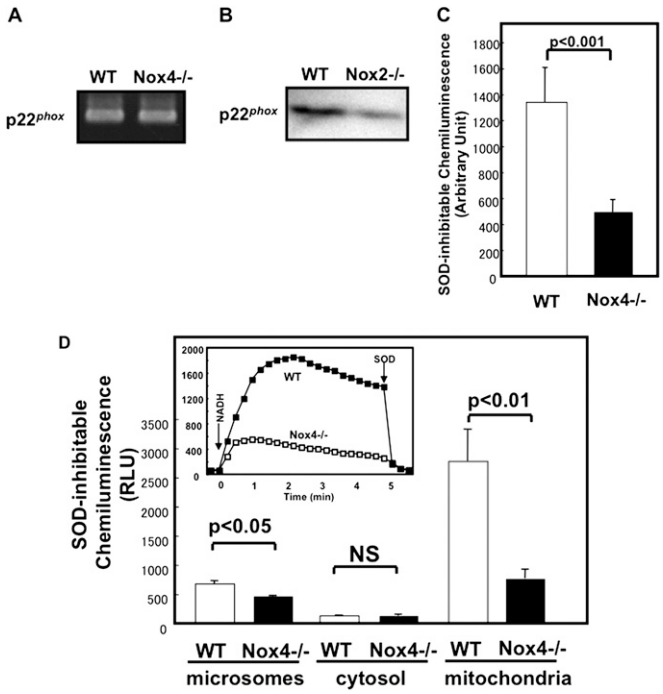


**Fig. S2.** Characteristics of c-*Nox4*$^{-/-}$ mice. (*A*) Expression of *p22*$^{phox}$ mRNA in the heart. Total RNA was isolated from WT and c-*Nox4*$^{-/-}$ mouse hearts and RT-PCR was performed with specific primers for *p22*$^{phox}$. (*B*) Expression of p22$^{phox}$ protein in the heart was evaluated by immunoblot analysis. (*C*) $O_2^-$ production in c-*Nox4*$^{-/-}$ mouse hearts. The level of $O_2^-$ production in the heart at baseline was evaluated by SOD-inhibitable lucigenin chemiluminescence. Note that $O_2^-$ production was significantly less in c-*Nox4*$^{-/-}$ mice than in WT mice. (*D*) Microsomal, cytosolic, and mitochondrial membrane fractions were prepared from WT and c-*Nox4*$^{-/-}$ mouse hearts. NADH-dependent and SOD-inhibitable $O_2^-$ release was measured by the lucigenin chemiluminescent method. Note that $O_2^-$ release from the mitochondrial membrane fraction was markedly reduced in c-*Nox4*$^{-/-}$ hearts compared with in WT mice. (*Inset*) Representative time courses of $O_2^-$ release from the mitochondrial membrane fractions prepared from WT and c-*Nox4*$^{-/-}$ mouse hearts. The SOD-inhibitable component of the $O_2^-$ release was quantitated. (*C* and *D*) Bar graphs indicate mean ± SEM obtained from three to five experiments.

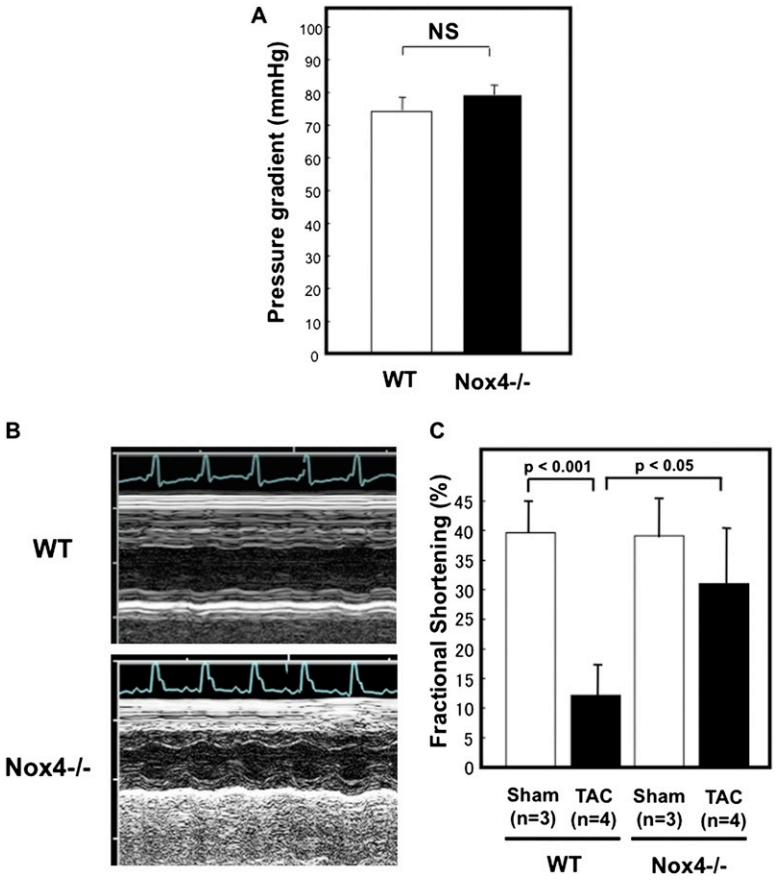


**Fig. S3.** LV function in c-*Nox4*$^{-/-}$ mice after TAC. c-*Nox4*$^{-/-}$ mice and WT littermates were subjected to TAC for 4 wk. (*A*) Pressure gradient 4 wk after TAC. The pressure gradient across the TAC was evaluated by hemodynamic measurements. Bar graph indicates mean ± SEM obtained from four experiments in each group. (*B*) LV systolic function 4 wk after TAC. Representative M-mode echocardiography images are shown. (*C*) Fractional shortening (%), an index of LV systolic function, was obtained echocardiographically.

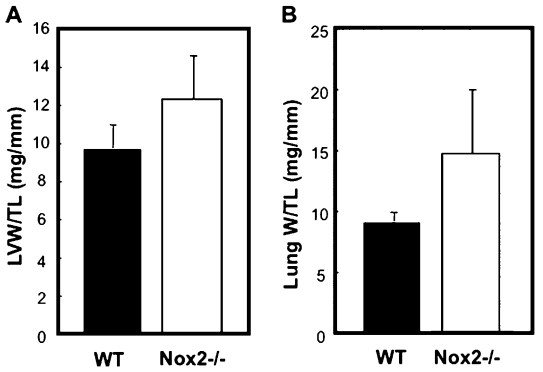


**Fig. S4.** The effect of TAC upon cardiac phenotype in *Nox2*$^{-/-}$ mice. Systemic *Nox2*$^{-/-}$ and WT mice were subjected to TAC for 4 wk. LVW/TL (*A*) and LungW/TL (*B*) were determined. Bar graphs indicate mean ± SEM obtained from five experiments.

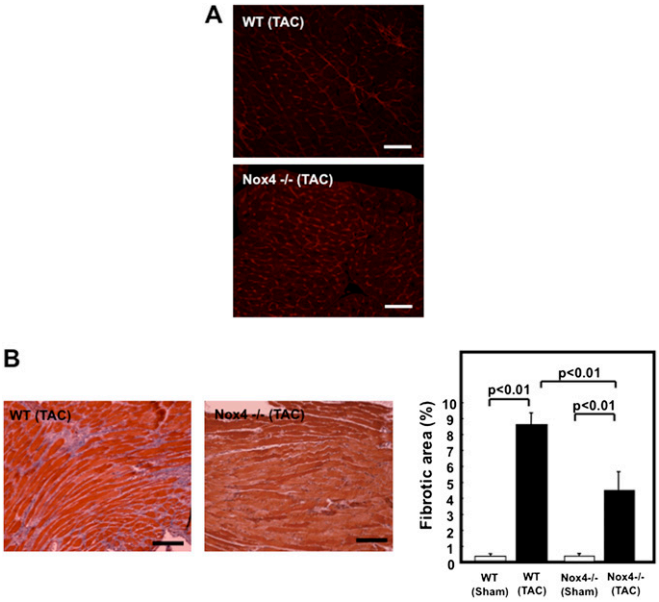


**Fig. S5.** The effect of TAC upon cardiac phenotype in c-*Nox4*$^{-/-}$ mice. c-*Nox4*$^{-/-}$ mice and WT littermates were subjected to either TAC for 4 wk or sham operation. Histological findings in c-*Nox4*$^{-/-}$ mouse hearts subjected to pressure overload. (*A*) LV cardiac myocyte cross-sectional area was measured using WGA staining. (Scale bars, 50 μm.) (*B*) LV fibrosis was evaluated by Masson's Trichrome staining. (Scale bars, 50 μm.) The bar graph indicates mean ± SEM obtained from three to five experiments.

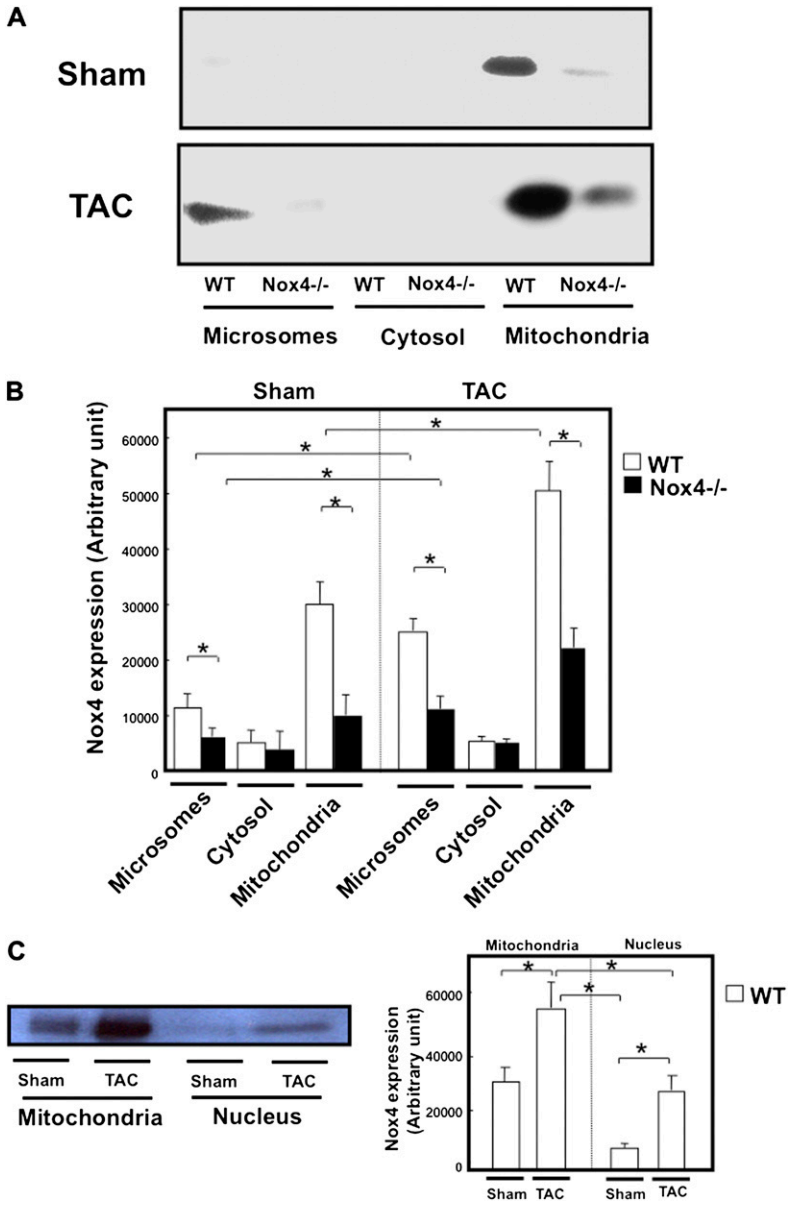


**Fig. S6.** The effect of pressure overload on Nox4 expression in microsomal, cytosolic, and mitochondrial subcellular fractions. Microsomal, cytosolic, mitochondrial, and nuclear fractions were prepared from c-*Nox4*$^{-/-}$ and WT mouse hearts subjected to either TAC for 4 wk or sham operation. (*A* and *C*) Expression of Nox4 was evaluated by immunoblot analyses using specific anti-Nox4 antibody. (*B* and *C*) Quantification of Nox4 expression (*$P < 0.05$). The bar graph indicates mean ± SEM from three experiments.

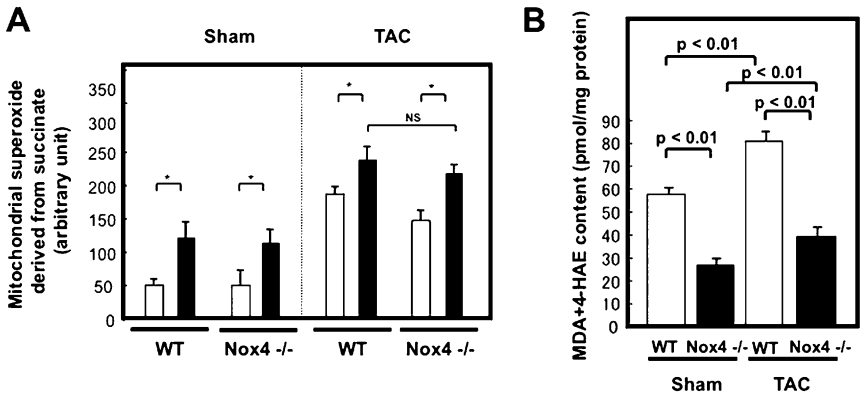


**Fig. S7.** The effect of TAC upon oxidative stress in c-*Nox4*$^{-/-}$ mice. (*A*) A mitochondrial fraction was freshly prepared from c-*Nox4*$^{-/-}$ mice and WT littermates subjected to either TAC for 4 wk or sham operation. The generation of $O_2^-$ from mitochondria was assessed by the lucigenin chemiluminescent method. Assays were conducted in the presence of succinate as a substrate of succinate-ubiquinone oxidoreductase (complex II) with or without antimycin A. Bar graphs indicate mean ± SEM obtained from three experiments (*$P < 0.05$). (*B*) MDA+4-HAE content was measured in cardiac tissue homogenates from WT and c-*Nox4*$^{-/-}$ mice. The bar graph indicates mean ± SEM obtained from four to five experiments.

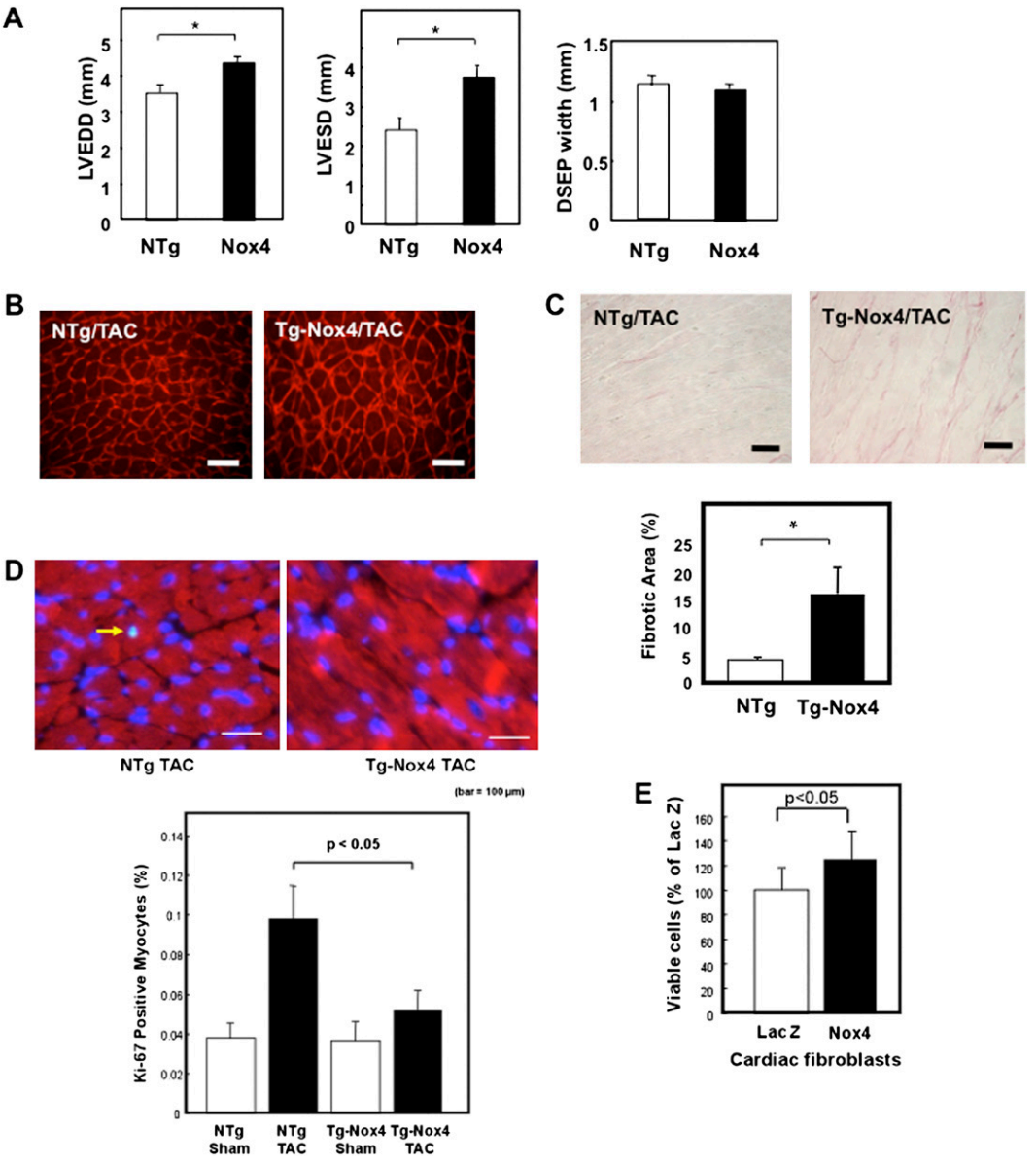


**Fig. S8.** The effects of aortic banding in Tg-*Nox4* mouse hearts. Tg-*Nox4* mice and NTg littermates were subjected to either TAC or sham operation for 2 wk. (*A*) Parameters of the left ventricle, including left ventricular end-diastolic dimension (LVEDD), left ventricular end-systolic dimension (LVESD), and diastolic septal width (DSEP width), were evaluated echocardiographically. (*B*) LV myocyte cross-sectional area was evaluated by WGA staining. (Scale bars, 50 μm.) (*C*) LV fibrosis was evaluated by picric acid sirius red staining. (Scale bars, 50 μm.) (*D*) The effect of TAC upon myocyte renewal was evaluated with anti-Ki67 staining. Costaining with antitroponin T antibody and quantitative analyses are shown. (*E*) The effect of Nox4 overexpression upon cell proliferation in cardiac fibroblasts. Adenoviruses harboring Nox4 and LacZ were transduced into cultured cardiac fibroblasts. After 72 h, the total cell number was assessed with the CellTiter Blue Cell Viability Assay. In *A*, *C*, *D* and *E*, bar graphs indicate mean ± SEM obtained from four to eight experiments (**P* < 0.05).

**Table S1. Echocardiographic analysis of c-*Nox4*$^{-/-}$ and *Nox 2*$^{-/-}$mice**

| | WT | c-*Nox4*$^{-/-}$ | WT | *Nox2*$^{-/-}$ |
|---|---|---|---|---|
| Age, mo | 3.6 ± 0.0 | 3.6 ± 0.0 | 3.5 ± 0.0 | 3.5 ± 0.0 |
| Body weight, g | 27.0 ± 3.0 | 26.7 ± 3.0 | 29.5 ± 1.0 | 29.6 ± 1.1 |
| Heart rate, bpm | 533.0 ± 42 | 555.2 ± 20 | 625.8 ± 9.0 | 608.2 ± 30.9 |
| DSEP WT, mm | 0.91 ± 0.19 | 1.00 ± 0.04 | 1.14 ± 0.07 | 1.21 ± 0.07 |
| LVEDD, mm | 3.61 ± 0.11 | 3.52 ± 0.21 | 2.90 ± 0.56 | 3.52 ± 0.52* |
| LVESD, mm | 2.17 ± 0.33 | 2.12 ± 0.29 | 1.99 ± 0.48 | 2.43 ± 0.56 |
| EF, % | 73.2 ± 8.2 | 70.5 ± 6.5 | 67.8 ± 6.2 | 67.0 ± 9.1 |
| FS, % | 39.9 ± 5.5 | 39.7 ± 6.0 | 31.9 ± 4.7 | 31.4 ± 6.6 |

DSEP WT, diastolic septal wall thickness; LVEDD, left ventricular end-diastolic dimension; LVESD, left ventricular end-systolic dimension; EF, ejection fraction; FS, fractional shortening.
**P* < 0.05 compared with WT.